$S_{17}(0)$ Determined from the Coulomb Breakup of 83 MeV/nucleon ^{8}B

B. Davids[1,2*], D.W. Anthony[1,3], T. Aumann[1‡], Sam M. Austin[1,2], T. Baumann[1], D. Bazin[1], R.R.C. Clement[1,2], C.N. Davids[4], H. Esbensen[4], P.A. Lofy[1,3], T. Nakamura[1†], B.M. Sherrill[1,2], and J. Yurkon[1]

[1] *National Superconducting Cyclotron Laboratory, Michigan State University, East Lansing, Michigan 48824*

[2] *Department of Physics and Astronomy, Michigan State University, East Lansing, Michigan 48824*

[3] *Department of Chemistry, Michigan State University, East Lansing, Michigan 48824*

[4] *Physics Division, Argonne National Laboratory, Argonne, Illinois 60439*

(January 23, 2001)

Abstract

A kinematically complete measurement was made of the Coulomb dissociation of ^{8}B nuclei on a Pb target at 83 MeV/nucleon. The cross section was measured at low relative energies in order to infer the astrophysical S factor for the ^{7}Be$(p,\gamma)^8$B reaction. A first-order perturbation theory analysis of the reaction dynamics including $E1$, $E2$, and $M1$ transitions was employed to extract the $E1$ strength relevant to neutrino-producing reactions in the solar interior. By fitting the measured cross section from E_{rel} = 130 keV to 400 keV, we find $S_{17}(0) = 17.8\ ^{+1.4}_{-1.2}$ eV b.

25.70.De, 26.20.+f, 26.65.+t, 27.20.+n

The β^+ decay of ^{8}B is the predominant source of high-energy solar neutrinos. These neutrinos produce the most events in the chlorine radiochemical detector at Homestake and the water and heavy water Cerenkov solar neutrino detectors SuperKamiokande and SNO. In the Sun, ^{8}B is produced via the ^{7}Be$(p,\gamma)^8$B reaction. Since 1964, the rate of this reaction has been the most uncertain input to the calculated solar neutrino fluxes, and the predicted event rates in solar neutrino detectors [1]. Precise knowledge of this reaction rate is essential not only for a detailed understanding of solar neutrino experiments, but also for constraining fundamental properties of neutrinos themselves. Direct measurements of the cross section are difficult because the target is radioactive, and the cross section small.

Radiative capture cross sections are often characterized in terms of an energy-dependent cross section factor, $S(E) = E\,\sigma(E)\,exp[2\pi Z_1 Z_2 e^2/(\hbar v)]$, where the Z_i are the charges and v the relative velocity of the nuclei involved. Hammache *et al.* [2] discuss the discrepancies in the overall normalizations of the direct measurements of the astrophysical S factor for the ^{7}Be$(p,\gamma)^8$B reaction, S_{17}. The disagreements among the direct measurements make an independent approach desirable. Peripheral transfer reactions that yield asymptotic normalization coefficients [3] and Coulomb breakup [4–10] permit the extraction of S factors with different systematic uncertainties. In the Coulomb breakup of ^{8}B, a virtual photon emitted by a heavy target nucleus such as Pb dissociates an incident ^{8}B projectile into ^{7}Be $+ p$. This is the inverse of the radiative capture reaction. The two reaction rates are related by the detailed balance theorem for photons of a given multipolarity.

As illustrated in [9], there is a disagreement in the energy dependence of the S factors extracted from the Coulomb dissociation experiments at RIKEN and GSI. Furthermore, the radiative capture reaction proceeds almost exclusively by $E1$ transitions at solar energies ($\approx$ 20 keV), but $E2$ and $M1$ transitions also play a role in Coulomb breakup for relative energies less than 1 MeV. $E2$ transitions are particularly important at low and intermediate beam energies, while $M1$ transitions are most significant at high incident beam energies. The contributions of these multipolarities to measured Coulomb dissociation cross sections must be correctly accounted for in order to obtain the $E1$ yield relevant to the production

of ^{8}B in the Sun. The size of the $M1$ contribution at low relative energies can be gauged from the direct measurement of the radiative capture cross section near the 0.64 MeV 1^+ resonance [11]. The $E2$ contribution to Coulomb dissociation cross sections was determined in an experiment by Davids *et al.* [12] in which the longitudinal momentum distributions of ^{7}Be fragments emitted in the Coulomb dissociation of intermediate energy ^{8}B projectiles on a Pb target were measured. In that experiment, we observed an asymmetry in the longitudinal momentum distribution of the emitted ^{7}Be fragments characteristic of interference between $E1$ and $E2$ transition amplitudes [13]. In this Letter, we report an exclusive breakup measurement that confirms the presence of $E2$ transitions in the Coulomb breakup, and quantitatively account for the measured $E2$ contribution in inferring $S_{17}(0)$.

We made a kinematically complete measurement of the cross section for the Coulomb dissociation of ^{8}B on a Pb target at low relative energies. An 83 MeV/nucleon ^{8}B beam delivered by the A1200 fragment separator [14] at the National Superconducting Cyclotron Lab impinged on a 47 mg cm^{-2} Pb target. The ^{8}B beam intensity was approximately 10^4 s^{-1}; nearly 4 billion nuclei struck the target. A 1.5 T dipole magnet separated the breakup fragments ^{7}Be and p from each other and from the elastically scattered ^{8}B nuclei, and dispersed the fragments according to their momenta. Four multiwire drift chambers (MWDCs) were used to measure the positions and angles of the breakup fragments after they passed through the magnet. An array of 16 plastic scintillators was used for particle identification. A thin scintillator at the exit of the A1200 provided continuous measurements of the beam intensity. In conjunction with the plastic scintillator array, it was also used to measure times-of-flight and to make intermittent beam transmission and purity measurements. A stainless steel plate prevented most of the direct ^{8}B beam from reaching the detectors. Using the ion optics code COSY INFINITY [15], we reconstructed the 4-momenta of the breakup fragments from the measured positions in the four detectors and the known magnetic field. The momentum calibration obtained from ^{7}Be and proton beams of known momenta was verified by checking that the fragment velocity distributions were centered about the beam velocity.

The detection efficiency and experimental resolution were determined by means of a Monte Carlo simulation, accounting for the beam emittance, energy loss and multiple scattering in the target and detectors, and the detector position resolution. The 1σ relative energy resolution ranged e.g. from 100 keV at $E_{rel} = 300$ keV to 250 keV at $E_{rel} = 1.5$ MeV. The 1σ resolution in the reconstructed angle of the dissociated ^{8}B projectile was 4.5 mrad. The dominant contribution to the experimental resolution was the position resolution of the MWDCs. The simulation of the angular distribution of the breakup fragments included both $E1$ and $E2$ transitions and anisotropic breakup in the ^{8}B center-of-mass system. Such an anisotropic angular distribution was predicted by the model of Ref. [13], and was required to fit the longitudinal momentum distributions of protons measured in the present experiment, and of ^{7}Be fragments measured in [12]. This point is addressed in detail below. The anisotropy is a consequence of interference between $E1$ and $E2$ transition amplitudes.

The results of [12] imply that a proper theoretical description of a ^{8}B Coulomb breakup experiment must include $E2$ transitions. In Ref. [12], the analysis of the measured ^{7}Be momentum distributions assumed first-order perturbation theory using the point-like projectile approximation for the Coulomb dissociation, and neglecting nuclear-induced breakup. This was reasonable for the experimental conditions considered, namely, for relatively small scattering angles of the ^{8}B center-of-mass. The analysis employed the $E1$ and $E2$ matrix elements predicted by the model of Ref. [13], scaled independently in order to reproduce the data. The best fits for both incident beam energies, 44 and 81 MeV/nucleon, were obtained when the ratio of the $E2$ and $E1$ matrix element scaling factors was 0.7. This was incorrectly reported as the ratio of the scaling factors for the $E2$ and $E1$ strength distributions; the correct value for this ratio is $0.7^2 = 0.49$. As a consequence, the reported [12] ratio of $E2$ and $E1$ S factors at $E_{rel} = 0.6$ MeV should be replaced by $4.7^{+2.0}_{-1.3} \times 10^{-4}$. The $E2$ strength extracted from the inclusive breakup measurement [12] is a factor of 10 to 100 larger than the upper limits reported in other experimental studies [7,9]. However, it is only slightly smaller than or in good agreement with recent theoretical calculations of $E2$ strength [13,16–19], and is consistent with the measurement of [20]. That the extracted experimental value should

be somewhat smaller than the theoretical values is consistent with the idea that first-order perturbation theory overestimates the $E2$ contribution to the cross section [13].

In order to minimize the role of $E2$ transitions and possible nuclear diffraction dissociation contributions to the breakup cross section measured in this experiment, only events with ^{8}B scattering angles of 1.8° or less were analyzed, corresponding classically to an impact parameter of 30 fm. Eikonal model [21] and distorted-wave Born approximation [22] calculations find that nuclear-induced breakup is negligible up to the grazing angle ($\approx 4°$), so the severe scattering angle cut imposed here gives confidence that nuclear effects are small, and that the point-like projectile approximation is valid. A first-order perturbation theory analysis neglecting nuclear-induced breakup was employed to interpret the results of this experiment. Such an approach is justified by the high beam energy and the restricted angular range covered in the experiment. Higher-order effects are most important at large scattering angles and low incident beam energies [10,13]. Recent continuum-discretized coupled channels calculations [23] suggest that nuclear excitations account for less than 4 % of our measured breakup cross section below 500 keV, and that higher-order electromagnetic processes have little effect on $d\sigma/dE_{rel}$ for the angles and energies covered in this experiment [24].

A particular strength of our analysis is that it includes all of the relevant electromagnetic multipole contributions, $E1$, $E2$, and $M1$. The procedure was the following. The $E1$ and $E2$ contributions were calculated using the structure model of Ref. [13], quenching the $E2$ matrix elements as discussed earlier. The $M1$ contribution at the 0.64 MeV 1^+ resonance was calculated by folding the measured $M1$ S factor [11] with the $M1$ photon spectrum calculated in 1st-order perturbation theory [25]. The contributions of the different multipolarities and their sum is shown in Fig. 1 (a). By requiring $\Theta_{^8B} \leq 1.8°$ and $E_{rel} \geq 130$ keV, we have ensured the dominance of $E1$ transitions. Except for a narrow range surrounding the $M1$ resonance, $E1$ transitions represent over 90% of the cross section in first-order perturbation theory. Fig. 1(b) shows the fraction of the measured cross section accounted for by $E1$ transitions in the present experiment.

The measured longitudinal momentum distribution of protons emitted in the Coulomb breakup of 83 MeV/nucleon ^{8}B on Pb with ^{8}B scattering angles of 1.8° or less is shown in Fig. 2. The 1σ proton momentum resolution was estimated from the simulation to be 4 MeV/c. Since the statistical significance of these data is less than that of the inclusive measurement reported in Ref. [12], we shall not use them to extract the $E2$ strength. Nevertheless, the asymmetry of this distribution is manifest. Also shown in the figure are calculations done with the model of Ref. [13], one with the full $E2$ strength, one with the $E2$ matrix elements scaled as described above, and another with no $E2$ matrix elements. The asymmetry observed in [12], taken together with momentum conservation, implies that the proton longitudinal momentum distribution must have a complementary asymmetry. We observed such an asymmetry for the first time in this measurement, confirming the presence of $E2$ transitions in the Coulomb breakup of ^{8}B.

In analyzing the measured decay energy spectrum, we convoluted the sum of the calculated $E1$, $E2$, and $M1$ contributions with the experimental resolution, and scaled the magnitude of the $E1$+$E2$ contribution in order to minimize χ^2 for the data points within two energy intervals, 130 keV to 2 MeV, and 130 to 400 keV. The factor by which the $E1$+$E2$ contribution was multiplied will be referred to as the normalization factor. The data above 2 MeV were excluded from the fit due to the presence of a 3^+ resonance at 2.2 MeV that was not included in the theoretical calculation, and because the statistics there are poor. At energies below 100 keV, our calculations show that the $E2$ component dominates, so these data were also excluded from the fit. A correction to the data for the feeding of the 429 keV excited state of ^{7}Be was made using the results of [7]. This correction is small, ranging from less than a percent at the lowest relative energies to about 10% around 2 MeV.

The best-fit normalization factor obtained for the data between 130 keV and 2 MeV with this procedure was $1.00\ ^{+0.02}_{-0.06}$. The 1σ error includes energy-dependent contributions from statistics, momentum and angular acceptance, detector efficiency, and the ^{7}Be excited state feeding correction. The various sources of systematic uncertainties include beam intensity (1%), target thickness (2.6%), momentum calibration (4.2%), and the theoretical uncertainty

(5.6%), resulting in a total systematic uncertainty of 7.5%. The theoretical uncertainty includes contributions from the size of the $E2$ component (2.5%) and from the extrapolation to zero energy (5%). Hence the result of the perturbation theory analysis of data from 130 keV to 2 MeV is $S_{17}(0) = 19.1\ ^{+1.5}_{-1.8}$ eV b.

A more reliable result can be obtained by analyzing a smaller relative energy range. Jennings *et al.* [26] point out that nuclear structure uncertainties increase significantly above $E_{rel} = 400$ keV. In order to minimize this model dependence, we also fit only the data between 130 keV and 400 keV. The theoretical extrapolation uncertainty is only 1% for this energy range [26]. The best-fit normalization factor for these data was $0.93\ ^{+0.05}_{-0.04}$, resulting in $S_{17}(0) = 17.8\ ^{+1.4}_{-1.2}$ eV b, with all sources of uncertainty added in quadrature. This result is consistent with the value extracted from all the data up to 2 MeV, implying that the simple potential model of Ref. [13] describes the physics well even at large relative energies, within the uncertainties. The data and the best-fit 1st-order perturbation theory calculations for all the data between 130 keV and 2 MeV, and for the data from 130 to 400 keV, convoluted with the experimental resolution, are shown in Fig. 3.

The present result is in good agreement with three of the capture measurements [2,11,27], and with the RIKEN (18.9 $\pm$ 1.8 eV b) and GSI (20.6 $\pm$ 1.2 $\pm$ 1.0 eV b) Coulomb breakup measurements [8,9]. It is also in excellent agreement with the results of asymptotic normalization coefficient determinations (17.3 $\pm$ 1.8 eV b) [3,28]. Although the results agree within the errors, the $E1$ strength found here is about 15% smaller than reported in the GSI Coulomb breakup measurement [9]. This might be ascribed to the neglect of $E2$ transitions in the analysis of the GSI measurement. The fraction of the breakup cross section attributable to $E2$ transitions depends on the energies and angles covered. In the present measurement, the experimental conditions were tailored to minimize the role of $E2$ transitions. The GSI measurement probed smaller impact parameters, implying in first-order perturbation theory a σ_{E2}/σ_{E1} ratio about 4 times larger than in this measurement throughout the relative energy range used to extract the S factor. Since the $E2$ contribution to the present measurement is about 5%, this could account for the difference between the ex-

tracted $E1$ components. Similarly, the S factor inferred from the RIKEN Coulomb breakup measurement [8] must be reduced by 4-15% [29] in order to account for the $E2$ contribution in 1st-order perturbation theory.

In summary, a kinematically complete measurement of the Coulomb dissociation of 83 MeV/nucleon ^{8}B on a Pb target was carried out using a dipole magnet to separate the breakup fragments from the beam. The Coulomb breakup cross section was measured at low relative energies and small ^{8}B scattering angles in order to infer the astrophysical S factor for the ^{7}Be$(p,\gamma)^8$B reaction with minimal complications from nuclear-induced breakup, $E2$ transitions, and higher-order electromagnetic effects. A first-order perturbation theory description of the reaction that included $E1$, $E2$, and $M1$ transitions, and a simple, single-particle ^{8}B structure model were used to interpret the measurement. The longitudinal momentum distribution of the emitted protons was measured and found to be asymmetric, consistent with our prior inclusive measurement of the ^{7}Be fragments, confirming the role of $E2$ transitions in the Coulomb breakup. Although we obtained data below 100 keV, they were excluded from the analysis because $E2$ transitions dominate at these energies. In order to minimize the theoretical uncertainties, the $E1$ strength in the Coulomb breakup was extracted from 130 to 400 keV, yielding $S_{17}(0) = 17.8\ ^{+1.4}_{-1.2}$ eV b. Having for the first time properly accounted for the $E2$ component, the dominant theoretical uncertainty in ^{8}B Coulomb breakup measurements, we have shown that direct radiative capture, Coulomb breakup and asymptotic normalization coefficient determinations give consistent values of $S_{17}(0)$.

This work was supported by the U.S. National Science Foundation; two of us (C.N.D. and H.E.) were supported by the U.S. Department of Energy, Nuclear Physics Division, under Contract No. W-31-109-ENG-38.

REFERENCES

* Present Address: Kernfysisch Versneller Instituut, Zernikelaan 25, 9747 AA Groningen, the Netherlands; email: davids@kvi.nl

‡ Present Address: Gesellschaft für Schwerionenforschung, Darmstadt, Germany

† Present Address: Department of Physics, Tokyo Institute of Technology, Tokyo, Japan

[1] J.N. Bahcall, S. Basu, and M.H. Pinsonneault, Phys. Lett. B **433**, 1 (1998).

[2] F. Hammache *et al.*, Phys. Rev. Lett. **80**, 928 (1998).

[3] A. Azhari *et al.*, Phys. Rev. Lett. **82**, 3960 (1999); Phys. Rev. C **60**, 055803 (1999).

[4] G. Baur, C.A. Bertulani, and H. Rebel, Nucl. Phys. A **458**, 188 (1986).

[5] J. Kiener *et al.*, Phys. Rev. C **44**, 2195 (1991).

[6] T. Motobayashi *et al.*, Phys. Rev. Lett. **73**, 2680 (1994).

[7] T. Kikuchi *et al.*, Phys. Lett. B **391**, 261 (1997).

[8] T. Kikuchi *et al.*, Eur. Phys. J. A **3**, 213 (1998).

[9] N. Iwasa *et al.*, Phys. Rev. Lett. **83**, 2910 (1999).

[10] G. Baur and H. Rebel, Annu. Rev. Nucl. Sci. **46**, 321 (1996).

[11] B.W. Filippone *et al.*, Phys. Rev. Lett. **50**, 412 (1983); Phys. Rev. C **28**, 2222 (1983).

[12] B. Davids *et al.*, Phys. Rev. Lett. **81**, 2209 (1998).

[13] H. Esbensen and G.F. Bertsch, Phys. Lett. B **359**, 13 (1995); Nucl. Phys. A **600**, 37 (1996).

[14] B.M. Sherrill *et al.*, Nucl. Instrum. Methods B **70**, 298 (1992).

[15] K. Makino and M. Berz, Nucl. Instrum. Methods A **427**, 338 (1999).

[16] S. Typel, H.H. Wolter, and G. Baur, Nucl. Phys. A **613**, 147 (1997).

[17] K. Bennaceur *et al.*, Nucl. Phys. A **651**, 289 (1999).

[18] P. Descouvement and D. Baye, Phys. Rev. C **60**, 015803 (1999).

[19] F. Barker, Nucl. Phys. A **660**, 249 (1999).

[20] V. Guimarães *et al.*, Phys. Rev. Lett. **84**, 1862 (2000).

[21] C.A. Bertulani and M. Gai, Nucl. Phys. A **636**, 227 (1998).

[22] R. Shyam and I.J. Thompson, Phys. Rev. C **59**, 2645 (1999).

[23] J.A. Tostevin, F.M. Nunes, and I.J. Thompson, Phys. Rev. C (to be published).

[24] B. Davids, Sam M. Austin, D. Bazin, H. Esbensen, B.M. Sherrill, I.J. Thompson, and J.A. Tostevin, Phys. Rev. C (submitted for publication).

[25] C.A. Bertulani and G. Baur, Phys. Rep. **163**, 299 (1988).

[26] B.K. Jennings, S. Karataglidas, and T.D. Shoppa, Phys. Rev. C **58**, 3711 (1998).

[27] F.J. Vaughn *et al.*, Phys. Rev. C **2**, 1657 (1970).

[28] A. Azhari *et al.*, Phys. Rev. C (to be published).

[29] T. Motobayashi, Nucl. Phys. A (to be published).

FIGURES

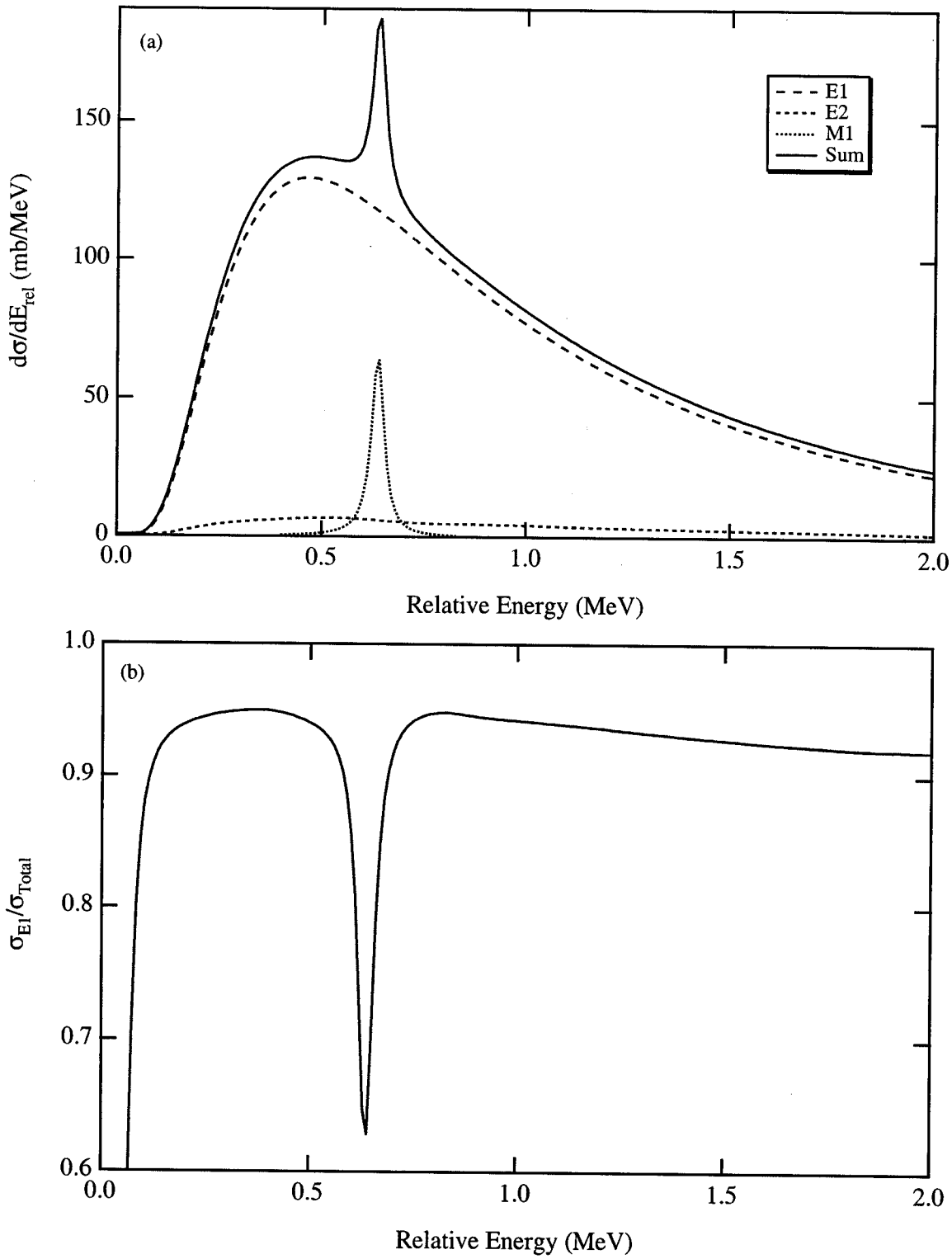
(a)
E1
E2
M1
Sum
150
100
50
0
0.0
0.5
1.0
1.5
2.0
dσ/dE_rel (mb/MeV)
Relative Energy (MeV)
(b)
1.0
0.9
0.8
0.7
0.6
0.0
0.5
1.0
1.5
2.0
σ_El/σ_Total
Relative Energy (MeV)

FIG. 1. (a) Contributions of $E1$, $E2$, and $M1$ transitions to the cross section for the Coulomb dissociation of 83 MeV/nucleon ^{8}B on Pb with ^{8}B scattering angles of 1.8° or less in 1st-order perturbation theory. $M1$, $E1$, and $E2$ cross sections are calculated as described in the text. (b) Fraction of the calculated cross section for the Coulomb dissociation of 83 MeV/nucleon ^{8}B on Pb with ^{8}B scattering angles $\leq$ 1.8° (b $\geq$ 30 fm) accounted for by $E1$ transitions in 1st-order perturbation theory.

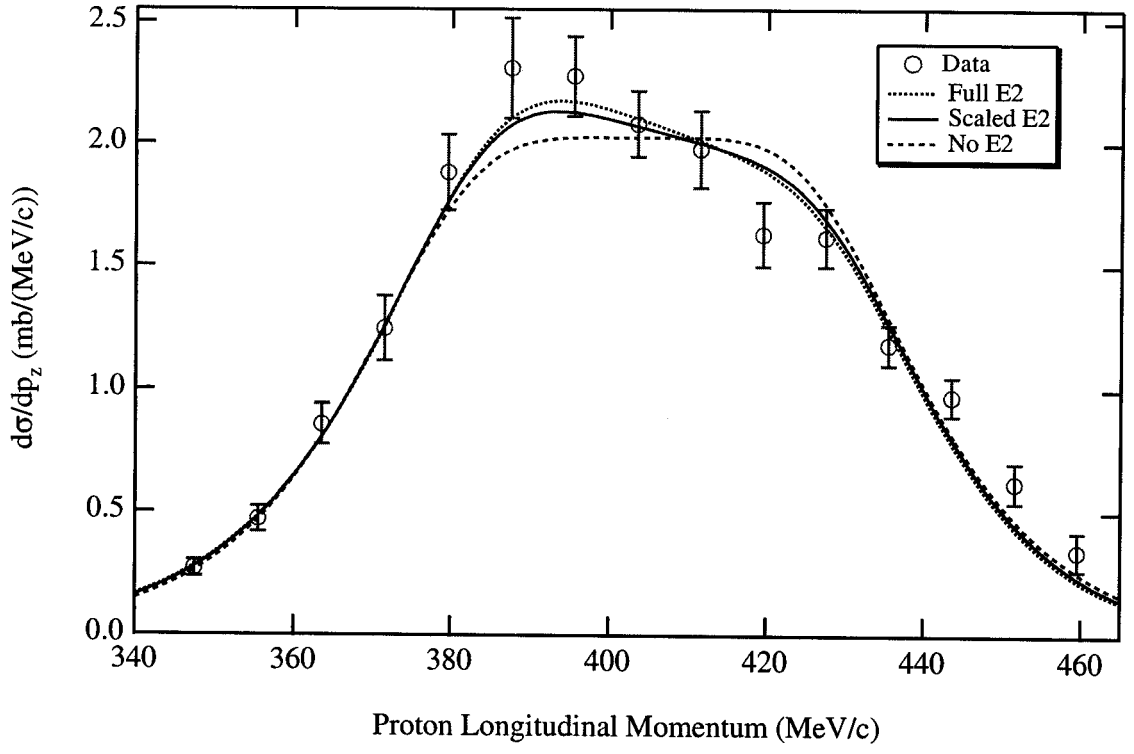

FIG. 2. Longitudinal momentum distribution of protons emitted in the Coulomb dissociation of 83 MeV/nucleon ^{8}B on Pb with ^{8}B scattering angles of 1.8° or less. The curves are 1st-order perturbation theory calculations using the model of Ref. [13] modified as described in the text, convoluted with the experimental resolution. The error bars indicate the size of the relative uncertainties.

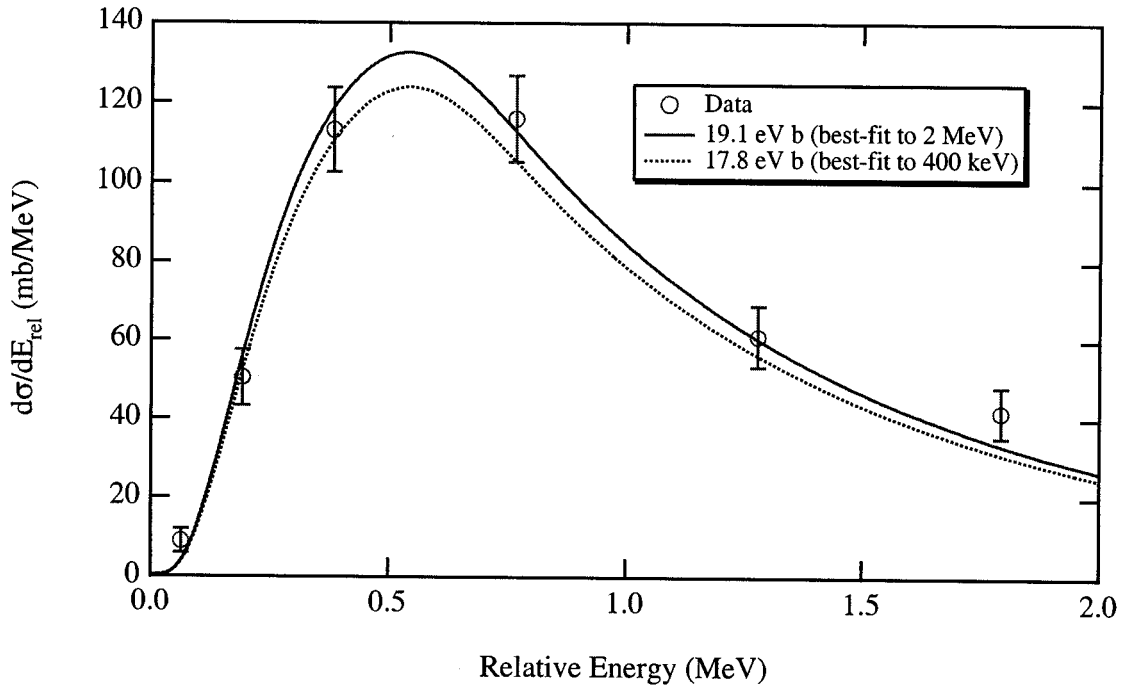

FIG. 3. Measured cross section for the Coulomb dissociation of 83 MeV/nucleon ^{8}B on Pb with ^{8}B scattering angles $\leq 1.8°$. Only relative errors are shown. Also depicted are the best-fit 1st-order perturbation theory calculations for the data between 130 keV and 2 MeV, and for the data between 130 keV and 400 keV, convoluted with the experimental resolution. The data point at 64 keV was excluded from the fit because of a large $E2$ contribution.

The following are the missing manuals from 1998-2000.

MSUCL1088
MSUCL1091
MSUCL1093
MSUCL1098
MSUCL1100
MSUCL1110--1112
MSUCL1129
MSUCL1133
MSUCL1138
MSUCL1144
MSUCL1147
MSUCL1151
MSUCL1154
MSUCL1163--1164
MSUCL1166
MSUCL1168--1169
MSUCL1173

ELSEVIER

Nuclear Physics A649 (1999) 153c–156c

NUCLEAR PHYSICS A

Exclusive studies of the GDR in excited nuclei

V. Nanal [a*], B.B. Back[a], D.J. Hofman[a], G. Hackman[a], D. Ackermann[a], S. Fischer[a], D. Henderson[a], R.V.F. Janssens[a], T.L. Khoo[a], A. A. Sonzogni[a], Y. Alhassid [b]

[a]Physics Division, Argonne National Laboratory,
9700 S Cass Avenue, Argonne, Illinois 60439, USA

[b]Center for Theoretical Physics, Sloane Physics Laboratory, Yale University,
New Heaven, Connecticut 06520, USA

The GDR in ^{164}Er at 62 MeV excitation energy has been studied in coincidence with the evaporation residues, selected using the Argonne fragment mass analyzer (FMA). The statistical model fit to the data indicate that ^{164}Er* has a prolate shape with deformation similar to the ground state.

1. Introduction

The giant dipole resonance (GDR) built on highly excited states of compound nuclei produced in heavy-ion induced fusion reactions has been used to study nuclear properties at high temperature. The nuclear deformations and shape changes have been deduced by studying the temperature and spin dependence of the width of the GDR in A$\sim$ 110 and $A \sim 160$ nuclei [1]. In addition to the γ rays of interest, the high-energy photon spectrum can have contributions from target contaminants (e.g. C, O) as well as from other competing processes like fission and deep-inelastic collisions, especially at high excitation energy and angular momentum. Although some attempts have been made to minimize these contaminant contributions, it has not been proven that such contributions are negligible in the inclusive experiments. A few exclusive measurements [2–4] have shown that the GDR spectrum gated with the residue is considerably narrower than the singles GDR spectrum, which may compromise the conclusions based on the inclusive results.

Recently, we have therefore carried out an experiment to measure the high energy γ–spectra in the compound nucleus ^{164}Er at 62 MeV excitation energy in coincidence with the evaporation residues, selected using the FMA, the results of which are reported here.

2. Experimental Details

The experiment was carried out using ^{40}Ar beam of 160 MeV from the ATLAS accelerator at Argonne National Laboratory on a 1 mg/cm^2 thick ^{124}Sn target. A rotating target holder was used to avoid excessive target heating. The high-energy photons were

*Present address: Tata Institute of Fundamental Research, Homi Bhabha Road, Colaba, Mumbai 400005, India

PII S0375-9474(99)00053-6

detected in the LEPPEX array while the evaporation residues were identified in the focal plane detector of the FMA.

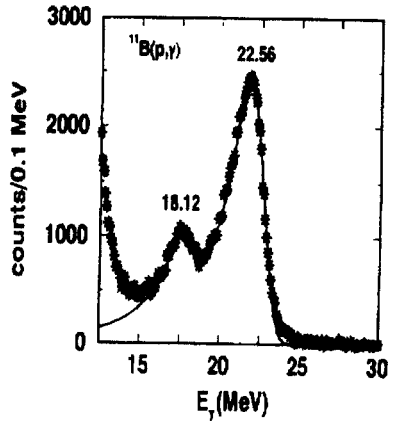

Figure 1. The high-energy peaks from the decay of the GDR in ^{12}C to the ground state (22.56 MeV) and the first excited state (18.12 MeV). A GEANT simulation spectrum (solid line) is also shown for comparison.

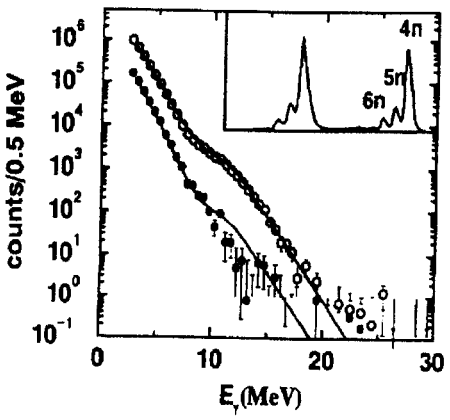

Figure 2. High energy γ-ray spectrum in the decay of ^{164}Er gated with A=160 (open circle) and A=159 (filled circle). The solid line is the statistical model fit (see text). Inset shows the mass spectrum obtained in the focal plane of the FMA.

The LEPPEX array consists of 16 large BaF_2 detectors ($5 \times 5 \times 25$ cm^3) surrounded by a plastic scintillator shield for cosmic ray rejection. The sub-nanosecond fast component of BaF_2 allows n-γ discrimination at a distance of 30 cm from the target. The response of the LEPPEX array was characterized using the standard ^{11}B(p,γ) (E_p =7.2 MeV) reaction to populate the GDR in ^{12}C which decays to the ground state with a 22.56 MeV γ−ray. The high-energy photons (22.56 MeV, 18.12 MeV) observed in this reaction, together with the low energy sources (0.898 MeV, 1.836 MeV and 6.13 MeV), provided the energy calibration over the entire region of 0-23 MeV. The observed energy resolution can be described as, $\frac{\Delta E}{E} \propto \frac{1}{E^{0.41}}$ with $\frac{\Delta E}{E}$ = 20% at 1 MeV. The experimental spectrum obtained with the ^{11}B(p,γ) reaction is shown in Figure 1. The simulated spectrum obtained from GEANT simulations is also shown for comparison. The observed line shape is well reproduced by adding a small exponential tail to the gaussian folding function as described in Ref. [5],

$$T(E) = Ce^{D(E-E_0)}(1 - e^{-(E-E_0)^2/2\sigma^2}) \qquad E < E_0 \tag{1}$$

where $C = 0.007E^{0.41}$ is the fraction of the peak from where the tail is added and $D = 0.21E^{0.41}$ is the slope of the exponential, E_0 and σ are the centroid and the width of the gaussian, respectively.

3. Results and Discussion

Figure 2 shows the high-energy γ ray spectrum in coincidence with A=160 (open circles) and A=159 (filled circles). The solid line in the figure is the calculation (best fit) using the statistical model code CASCADE [6] after folding with the detector response, as explained in the previous section. The CASCADE output cannot be directly compared with the residue gated experimental spectrum. We have therefore followed the approximate procedure of Van Schagen et al. [7] to generate the equivalent theoretical spectrum from CASCADE. The total fusion cross section was taken from the data of Reisdorf et al. [8] and the initial angular distribution was derived using the extra-extra push model [9]. We have assumed the classical sum rule (100%). The GDR parameters, centroid energy, deformation and width of the two components, were allowed to vary in order to get best fit. The calculated CASCADE spectrum for the 4n decay channel was normalized to data in the low energy region (5-7 MeV). The χ^2 in the GDR region was then determined for this 'normalized' spectrum and parameters were varied to minimize this χ^2. The best fit parameters are shown in Table 1. It should be noted that the high-energy tail of GDR is very sensitive to the level density parameter 'a'. We have used a=A/7.5. Figure 2 also shows the calculated GDR spectrum for the 5n decay channel with best fit parameters obtained from the 4n decay channel together with the data.

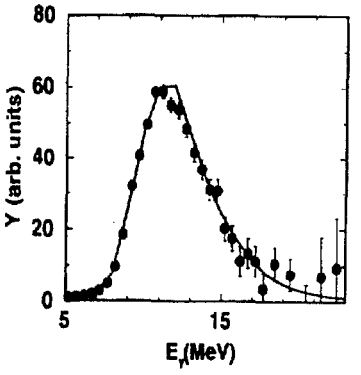

Figure 3. Divided plots (see text) for the experimental data together with the statistical model fit (solid line). The ordinate Y is proportional to photoabsorption cross section.

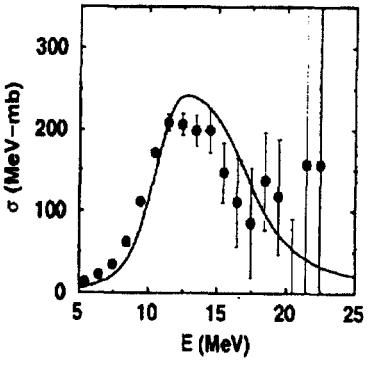

Figure 4. The absorption cross section obtained from the best fit to the data is compared with a thermal shape fluctuation calculation for $J = 44\hbar$, T_{eff}= 1.0 MeV, E_{av} = 13.8 MeV.

Figure 3 shows the data and the best fit divided by a calculated spectrum obtained with a constant E1 strength on a linear scale for better visualization.

In Figure 4, the absorption cross section corresponding to the GDR parameters for the best fit is compared with that based on thermal shape fluctuation calculations [10] for E_{av} = 13.8 MeV (as obtained from the fit to data), J=44 $\hbar$ and the effective final temperature of 1.0 MeV. It can be seen that the theory does not describe data very well. The reasons for this discrepancy will be investigated.

Table 1
Fit parameters for ^{124}Sn(^{40}Ar, 4n) at E^*=62 MeV, l_{max}= 47$\hbar$. The errors are obtained from a χ^2 analysis of the fit.

S_1	E_1 MeV	Γ_1 MeV	S_2	E_2 MeV	Γ_2 MeV	E_{av} MeV
0.4(.05)	11.9(0.3)	3.6(0.4)	0.6(0.07)	15.1(0.3)	6.4(0.8)	13.8(0.4)

4. Conclusion

In conclusion, we have studied the GDR in ^{164}Er at 62 MeV excitation energy gated with the residue ^{160}Er. We find that ^{164}Er has a prolate shape at T$\sim$1 MeV with a deformation similar to the ground state with $\beta = 0.27 \pm 0.02$. The GDR centroid energy is consistent with ground state systematics. A further analysis using a Monte Carlo Cascade code is in progress. Also incoroparting theoretical strength function into cascade for different E^* and J values will provide a better comparison with the theory.

This work was supported by the U.S. Department of Energy, Nuclear Physics Division, under contract No. W-31-109-ENG-38.

REFERENCES

1. J. J. Gaardhøje, Ann. Rev. of Nucl. Sci. 42, (1992) 483.
2. A. Atac et al. Phy. Lett. B 252, (1990) 545.
3. R. Noorman et al. Phys. Lett.B 292, (1992) 257.
4. M. Mattiuzzi et al. Nucl. Phys. A 612, (1997) 262.
5. M. T. Collins et al. Phys. Rev. C26 (1982) 332.
6. F. Puhlhofer, Nucl. Phys. A 280 (1977)267.
7. J. Van Schagen et al. Nucl. Phys. A 581 (1995) 145.
8. Reisdorf et al. Nucl. Phys. A 438 (1985) 222.
9. W. Q. Shen et al. Phys. Rev. C 36 (1987) 115.
10. Y. Alhassid et al. Nucl. Phys. A 509 (1990) 461.